Structural Engineering and Mechanics, Vol. 21, No. 2 (2005) 121-136
DOI: http://dx.doi.org/10.12989/sem.2005.21.2.121

A general convergence condition of the Newton-Raphson algorithm applied to compressible hyperelasticity

François Peyraut†

Laboratoire Mécatronique3M, Université de Technologie de Belfort-Montbéliard, Sévenans, 90010 Belfort cedex, France

Zhi-Qiang Feng‡

Laboratoire de Mécanique d'Evry, Université d'Evry-Val d'Essonne, 40, rue du Pelvoux, 91020 Evry cedex, France

Nadia Labed‡†

Laboratoire Mécatronique3M, Université de Technologie de Belfort-Montbéliard, Sévenans, 90010 Belfort cedex, France

(Received December 8, 2004, Accepted June 21, 2005)

Abstract. This paper presents the implementation of the Blatz-Ko hyperelastic compressible model in a finite element program to deal with large deformation problems. We show analytically and numerically that the minimum number of increment steps in the Newton-Raphson algorithm depends on material properties and applied loads. We also show that this dependence is related to the orientation preservation principle. So we propose a convergence criteria based on the sign of eigenvalues of the deformation gradient matrix.

Key words: Blatz-Ko model; hyperelasticity; finite element; large deformation; Newton-Raphson.

1. Introduction

Today, the compressible hyperelasticity causes many interrogations. In particular, existence and uniqueness of the solution are not always satisfied (Ciarlet 1988). In addition, loss of ellipticity of equilibrium equations (Horgan 1996) can involve numerical difficulties near the breaking values of loading (Wineman 1995). In addition, for the Blatz-Ko hyperelastic compressible model (Blatz and Ko 1962), the violation of orientation preservation can cause the incremental Newton-Raphson algorithm to diverge (Peyraut 2003a). Indeed, if a deformation with a negative determinant of the deformation gradient matrix cannot be reached by a continuous process starting from the reference

† Professor, Corresponding author, E-mail: francois.peyraut@utbm.fr
‡ Professor, E-mail: feng@iup.univ-evry.fr
‡† Associate Professor, E-mail: nadia.labed@utbm.fr

configuration, it is possible to reach it with a numerical discontinuous process. More precisely, if the loading increment is too large, the incremental Newton-Raphson algorithm can cause a discontinuous jump between two branches of the equilibrium curve. In this case, the successive tangents do not allow a return to the acceptable branch where the physical solution is located. The Newton-Raphson algorithm then fails to converge (i.e., the iteration count is infinite or the iterative process stops with an error message), otherwise the algorithm would converge to a physical non-admissible solution on the non-admissible branch.

In order to prevent Newton-Raphson divergence, we propose to control the orientation preservation by using the sign of the eigenvalues of the deformation gradient matrix. A negative or null eigenvalue is indeed symptomatic of an orientation preservation loss. Within the framework of the finite element theory, this control must be carried out at the Gauss points and for each Newton-Raphson's iteration. Its implementation in the finite element software FER is presented in this paper.

We have successfully tested this numerical orientation preservation control in two cases. The first one concerns the one dimensional case of a hyperelastic cube subjected to a compressive force in a rigid container. Friction in contact with the side walls is supposed to be negligible and cube bases perfectly stuck on the container bottom. The results are in very good agreement with the optimal loading step number analytically calculated in (Peyraut 2001). This optimal loading step number is as small as possible to minimize computing time but sufficiently large to ensure the Newton-Raphson algorithm to converge. The second case relates to the more general case of a 3D structure. This structure is made of a rectangular hyperelastic specimen subjected to a uniform pressure on its upper and lower sides. As in the first case, the numerical results are in very good agreement with the optimal loading step number analytically calculated in (Peyraut 2003b).

2. Blatz-Ko constitutive law

Rubber or other polymer materials are said to be hyperelastic. Usually, these kind of materials undergo large deformations. Let $\mathbf{x}$ and $\mathbf{X}$ denote the position vectors of a particle P in the current and reference configurations of a deformable body (Fig. 1).

If we consider the framework of large deformations in stationary mode (static calculation) with Lagrangian description, the motion of this body is specified by a smooth vector function $\mathbf{x} = \Phi(\mathbf{X})$. It is usual to introduce the displacement vector $\mathbf{U}$ such that

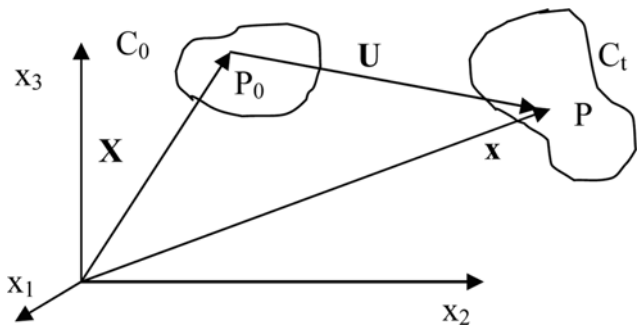

Fig. 1 Configurations

$$\mathbf{x} = \Phi(\mathbf{X}) = \mathbf{X} + \mathbf{U} \tag{1}$$

In the context of finite elements, displacements of structures **U** are given by the product of shape functions and nodal displacements:

$$\mathbf{U} = \mathbf{N}\,\mathbf{u} \tag{2}$$

where **N** is the matrix of shape functions and **u** is the vector of nodal displacements. In order to describe the geometrical transformation at the particle *P*, the deformation gradient tensor is introduced by

$$\mathbf{F}_{ij}(\mathbf{X}) = \frac{\partial \Phi_i(\mathbf{X})}{\partial \mathbf{X}_j} = \frac{\partial \mathbf{x}_i}{\partial \mathbf{X}_j} = \delta_{ij} + \frac{\partial \mathbf{U}_i}{\partial \mathbf{X}_j} \tag{3}$$

Because of large displacements and rotations, Green-Lagrangian strain is adopted for the nonlinear relationships between strains and displacements. One notes **C** the stretch tensor or the right Cauchy-Green deformation tensor ($\mathbf{C} = \mathbf{F}^T\mathbf{F}$). The Green-Lagrangian strain tensor **E** is defined by

$$\mathbf{E} = (\mathbf{C} - \mathbf{I})/2 \tag{4}$$

In the case of hyperelastic law, there exists an elastic potential function *W* (or strain energy density function) which is a scale function of one of the strain tensors, whose derivative with respect to a strain component determines the corresponding stress component. This can be expressed by

$$\mathbf{S}_{ij} = \frac{\partial W}{\partial \mathbf{E}_{ij}} = 2\frac{\partial W}{\partial \mathbf{C}_{ij}} \tag{5}$$

where **S** is the second Piola-Kirchoff stress tensor.

In the particular case of isotropic hyperelasticity (Ciarlet 1988), Eq. (5) can be written by

$$\mathbf{S} = 2\left[I_3\frac{\partial W}{\partial I_3}\mathbf{C}^{-1} + \left(\frac{\partial W}{\partial I_1} + I_1\frac{\partial W}{\partial I_2}\right)\mathbf{Id} - \frac{\partial W}{\partial I_2}\mathbf{C}\right] \tag{6}$$

where **Id** is the unity tensor and I_i (i = 1, 2, 3) denote the invariants of the right Cauchy-Green deformation tensor **C**:

$$I_1 = \mathbf{C}_{ii}\ ;\ I_2 = (I_1^2 - \mathbf{C}_{ij}\,\mathbf{C}_{ij})/2\ ;\ I_3 = det\,(\mathbf{C}_{ij}) \tag{7}$$

The Blatz-Ko constitutive law is used to model compressible foam-type polyurethane rubbers (Blatz and Ko 1962). The strain energy density function is given as follows

$$W = \frac{\mu}{2}\left[\frac{I_2}{I_3} + 2\sqrt{I_3} - 5\right] \tag{8}$$

where $\mu = E/2(1+\nu)$ is the shear modulus. E and ν are respectively Young's modulus and Poisson's ratio. It is worth noting that the Poisson's ratio is equal to 0.25 in the particular case of Blatz-Ko material. By deriving the energy density (8) with respect to the three invariants, we obtain

$$\frac{\partial W}{\partial I_1} = 0;\ \frac{\partial W}{\partial I_2} = \frac{\mu}{2}\frac{1}{I_3};\ \frac{\partial W}{\partial I_3} = \frac{\mu}{2}\left[-\frac{I_2}{I_3^2} + \frac{1}{\sqrt{I_3}}\right] \tag{9}$$

Reporting the result in Eq. (6) and using the Cayley-Hamilton theorem gives

$$\mathbf{S} = \mu \mathbf{F}^{-1} \{ \sqrt{I_3} \mathbf{Id} - \mathbf{B}^{-1} \} \mathbf{F}^{-T} \tag{10}$$

where $\mathbf{B} = \mathbf{F}\mathbf{F}^T$ is the left Cauchy-Green deformation tensor associated to $\mathbf{F}$.

Classically, the Cauchy stress (or true stress) tensor σ can be calculated from the second Piola-Kirchoff stress tensor $\mathbf{S}$ as follows:

$$\sigma = \frac{1}{det(\mathbf{F})} \mathbf{F}\mathbf{S}\mathbf{F}^T \tag{11}$$

3. Finite element formulation of nonlinear structures

In the linear analysis, a linear relation is assumed between strains and displacements. However, if there are large displacements and strains, such as in the case of rubber applications, the nonlinear relation between strains and displacements on one hand and between stresses and strains on the other hand cannot be ignored. Also, the equilibrium equation of internal and external forces should be considered in the deformed configuration. The geometrically nonlinear analysis may be described by using the total or the updated Lagrangian formulations. The total Lagrangian formulation is derived with respect to the initial configuration. The updated Lagrangian formulation is derived with respect to the current configuration. In other words, the total Lagrangian formulation constructs the tangent stiffness matrix with respect to the initial configuration. On the other hand, the updated Lagrangian formulation constructs the tangent stiffness matrix with respect to the current configuration. The updated Lagrangian formulation is computationally effective (Bathe 1979) because it does not include the initial displacement matrix. In the total Lagrangian formulation, the initial configuration remains constant. This simplifies the computation (Wood 1977). Therefore, the total Lagrangian formulation was selected in this work for the finite element discretization (Belytschko 2000). According to Eqs. (2-4), the Green-Lagrangian strain includes formally linear and nonlinear terms in function of nodal displacements

$$\mathbf{E} = (\mathbf{B}_L + \mathbf{B}_{NL}(\mathbf{u}))\, \mathbf{u} \tag{12}$$

where $\mathbf{B}_L$ is the matrix which relates the linear strain term to the nodal displacements, and $\mathbf{B}_{NL}(\mathbf{u})$, the matrix which relates the nonlinear strain term to the nodal displacements. From Eq. (12), the incremental form of the strain-displacement relationship is

$$\delta\mathbf{E} = (\mathbf{B}_L + \mathbf{B}_{NL}(\mathbf{u}))\, \delta\mathbf{u} \tag{13}$$

Using the principle of virtual displacement, the virtual work δW is given as

$$\delta W = \int_{V_0} \mathbf{S}\delta\mathbf{E} dV_0 - \mathbf{F}_{ext}\delta\mathbf{u} \tag{14}$$

where V_0 is the volume of the initial configuration and $\mathbf{F}_{ext}$, the vector of external loads.

From Eqs. (5-10), one obtains

$$\delta\mathbf{S} = \mathbf{D}\ \delta\mathbf{E} = \mathbf{D}\ (\mathbf{B}_L + \mathbf{B}_{NL}(\mathbf{u}))\ \delta\mathbf{u} \tag{15}$$

where $\mathbf{D}$ is the current fourth order stress-strain tensor. The stress-strain tensor's coefficients are obtained by deriving (10) with respect to the Green-Lagrange strain tensor E:

$$D_{ijkl} = \mu\{-2J(2\mathbf{E}+\mathbf{Id})^{-1}_{ik}(2\mathbf{E}+\mathbf{Id})^{-1}_{lj} + J(2\mathbf{E}+\mathbf{Id})^{-1}_{lk}(2\mathbf{E}+\mathbf{Id})^{-1}_{ij} + 2[(2\mathbf{E}+\mathbf{Id})^{-1}_{ik}(2\mathbf{E}+\mathbf{Id})^{-2}_{lj} + (2\mathbf{E}+\mathbf{Id})^{-2}_{ik}(2\mathbf{E}+\mathbf{Id})^{-1}_{lj}]\} \quad (16)$$

Substituting $\delta\mathbf{E}$ from Eq. (13) into Eq. (14) results in

$$\delta W = \int_{V_0} \mathbf{S}(\mathbf{B}_L + \mathbf{B}_{NL}(\mathbf{u}))\delta\mathbf{u}dV_0 - \mathbf{F}_{ext}\delta\mathbf{u} = (\mathbf{F}_{int} - \mathbf{F}_{ext})\delta\mathbf{u} \quad (17)$$

where the vector of internal forces is defined by

$$\mathbf{F}_{int} = \int_{V_0} (\mathbf{B}_L + \mathbf{B}_{NL}(\mathbf{u}))^T \mathbf{S}dV_0 \quad (18)$$

Since $\delta\mathbf{u}$ is arbitrary, a set of nonlinear equations can be obtained as

$$\mathbf{F}_{int} - \mathbf{F}_{ext} = 0 \quad (19)$$

Eq. (19) is strongly non-linear, because of finite strains and large displacements of solid. A typical solution procedure for this type of nonlinear analysis is obtained by using the Newton-Raphson iterative procedure (Belytschko 2000)

$$\begin{cases} \mathbf{K}^i_T \Delta\mathbf{u} = \mathbf{F}_{ext} - \mathbf{F}^i_{int} \\ \mathbf{u}^{i+1} = \mathbf{u}^i + \Delta\mathbf{u} \end{cases} \quad (20)$$

where i and $i+1$ are the iteration numbers at which the equations are computed. $\mathbf{K}^i_T$ is the tangent stiffness matrix, $\mathbf{u}$, the vector of nodal displacements, $\Delta\mathbf{u}$, the vector of nodal displacements correction, and $\mathbf{F}^i_{int}$, the vector of internal forces. Taking the derivative of $\mathbf{F}_{int}$ with respect to the nodal displacements $\mathbf{u}$ gives the tangent stiffness matrix as

$$\mathbf{K}_T = \frac{\partial \mathbf{F}_{int}}{\partial \mathbf{u}} = \int_{V_0} \left(\frac{\partial \mathbf{S}}{\partial \mathbf{u}} (\mathbf{B}_L + \mathbf{B}_{NL}(\mathbf{u})) + \mathbf{S}\frac{\partial \mathbf{B}_{NL}(\mathbf{u})}{\partial \mathbf{u}} \right) dV_0 \quad (21)$$

In addition, this expression can be written by substituting Eq. (11) into Eq. (13) as

$$\mathbf{K}_T = \int_{V_0} \mathbf{B}^T_L \mathbf{D}\mathbf{B}_L dV_0 + \int_{V_0} \mathbf{S}\frac{\partial \mathbf{B}_{NL}(\mathbf{u})}{\partial \mathbf{u}} dV_0 + \int_{V_0} (\mathbf{B}^T_L \mathbf{D}\mathbf{B}_{NL} + \mathbf{B}^T_{NL}\mathbf{D}\mathbf{B}_L + \mathbf{B}^T_{NL}\mathbf{D}\mathbf{B}_{NL}) dV_0$$
$$= \mathbf{K}_E + \mathbf{K}_\sigma + \mathbf{K}_U \quad (22)$$

In Eq. (22), the first term is the elastic stiffness matrix $\mathbf{K}_E$, the second term is the geometric stiffness (or initial stress stiffness) matrix $\mathbf{K}_\sigma$, and the third term is the initial displacement stiffness matrix $\mathbf{K}_U$. This formulation has been implemented in an object-oriented finite element code named FER.

4. Orientation preservation control in Newton-Raphson iterative procedure

Usually, the orientation preservation is tested with the determinant of the deformation gradient $\mathbf{F}$. If $det(\mathbf{F})$ is positive, the orientation is preserved and if $det(\mathbf{F})$ is null or negative, the orientation preservation is lost. In this section, we will show that a control based on the $\mathbf{F}$ eigenvalues is more

efficient. In order to demonstrate that, let us consider the three **F** eigenvalues, noted λ_1, λ_2 and λ_3. These eigenvalues can be positive, negative, null or complex (in this last case, two eigenvalues are necessarily conjugated and the third one is real). At the current iteration of Newton-Raphson procedure, seven cases can occur:

- Case 1: all eigenvalues are positive: $\lambda_1 > 0$; $\lambda_2 > 0$; $\lambda_3 > 0$
- Case 2: two eigenvalues are conjugate complex numbers and the third one is positive (for instance: $\lambda_1 = \bar{\lambda}_2; \lambda_3 > 0$)
- Case 3: two eigenvalues are negative and the third one is positive (for instance: $\lambda_1 < 0$; $\lambda_2 < 0$; $\lambda_3 > 0$)
- Case 4: there exists at least one null eigenvalue (for instance: $\lambda_1 = 0$)
- Case 5: two eigenvalues are positive and the third one is negative (for instance: $\lambda_1 > 0$; $\lambda_2 > 0$; $\lambda_3 < 0$)
- Case 6: all eigenvalues are negative $\lambda_1 < 0$; $\lambda_2 < 0$; $\lambda_3 < 0$
- Case 7: two eigenvalues are conjugate complex numbers and the third one is negative (for instance: $\lambda_1 = \bar{\lambda}_2; \lambda_3 < 0$)

The determinant of **F** is the product of eigenvalues

$$det(\mathbf{F}) = \lambda_1 \lambda_2 \lambda_3 \tag{23}$$

This determinant is strictly positive for cases 1 to 3 and negative or null for cases 4 to 7. That means that orientation will not be preserved if one of cases 4 to 7 occurs. The current iteration of the Newton-Raphson algorithm is then not acceptable and the procedure must be stopped.

Case 3 is also not available although the determinant of **F** is positive. Indeed, it corresponds to a surface reversal without physical meaning (see appendix for details about the reversal problem). So, Case 3 can not be accepted.

In conclusion, the current iteration must be rejected if cases 3-7 are detected. These cases are characterized by a negative or null eigenvalue of **F**. In order to prevent Newton-Raphson divergence, we then propose to control the orientation preservation by using the sign of the eigenvalues of deformation gradient **F**. Within the framework of the finite element theory, this control must be carried out at the Gauss points and for each Newton-Raphson's iterations. The procedure control is written as follows in the finite element software FER (Box 1).

Given: element node coordinates xyz, displacements vector disp
For each Gauss integration point:
a) compute the derivation of shape functions with respect to reference coordinates deriv
b) compute the Jacobian matrix: J=deriv*xyz
c) compute the derivation of shape functions with respect to real coordinates: dndx= J^{-1}*deriv
d) compute the derivation of displacements with respect to real coordinates: dispdx=dndx*disp;
e) compute the deformation gradient matrix: F=dispdx+Id
f) compute the eigenvalues of F
g) check the sign of eigenvalues, if cases 3-7, Newton-Raphson procedure is then stopped.
h) restart with more load steps.

Box 1. Orientation preservation control in Newton-Raphson solution procedure

The approach presented on Box 1 does not depend on the material constitutive law because only eigenvalues of the deformation gradient are required. This approach is thus very general and could be applied not only to Blatz-Ko materials but also to other materials of slightly or largely compressible behavior.

From a computational point of view, the proposed approach is the most efficient method to deal with the orientation preserving problem in the framework of Newton-Raphson algorithm. The restart process (Step *h*) is indeed performed with a load step number selected so as to approach as closely as possible to the orientation preserving limit. Beyond this limit, negative volume, negative area or negative length can occur. Step *h* provides thus an optimal load step number associated with the minimal computational cost. If the optimal load step number is reduced just by one, Newton-Raphson algorithm will diverge as it will be shown in sections 5.1 and 5.2.

5. Numerical examples

5.1 One dimensional example

In this section, we study the particular case of a hyperelastic cube subjected to a compressive pressure p in a rigid container. Friction in contact with the sidewalls is supposed to be negligible and cube bases perfectly stuck on the container bottom (Fig. 2). The displacements in the (x, y) plane are then equal to zero:

$$u_x = u_y = 0 \tag{24}$$

Besides, the vertical displacement u_z only depends on z in a linear form:

$$u_z(z) = \frac{U}{H} z \tag{25}$$

where U represents the vertical displacement on the top of the cube ($z = H$). The studied problem is consequently one-dimensional.

The loss of orientation preservation can cause the incremental Newton-Raphson algorithm to diverge (Peyraut 2001). In order to ensure at the same time the convergence and orientation preservation, a progressive increase of the loading step number n constitutes a possible strategy. This strategy consists in restarting the computation with an increase of n if Newton-Raphson

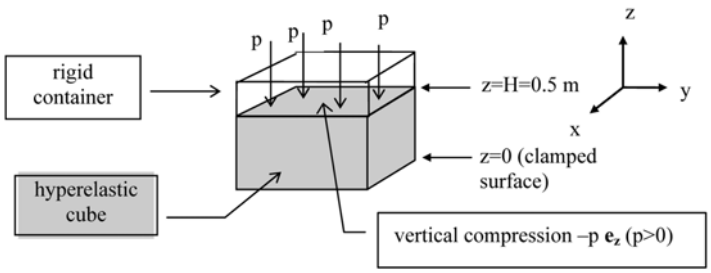

Fig. 2 Compression of a cube in a rigid container

divergence is detected. But this strategy is expensive because previous calculations are lost. It is thus interesting to seek the optimal incremental loading number n allowing convergence without restarting. In order to find this optimal loading number, we first study the relation between displacements and loading. This relation can be obtained thanks to the minimization of the total potential energy

$$I(u) = \int_{\Omega} W d\Omega + \int_{S} p u_z dS \tag{26}$$

The first integral is calculated over the volume Ω of the cube while the second is calculated on the top surface S of the cube. If we use the displacement field given by Eqs. (24, 25) in connection with Eq. (8), the energy density is

$$W = \frac{\mu}{2}\left\{\left(1 + \frac{U}{H}\right)^{-2} + 2\frac{U}{H} - 1\right\} \tag{27}$$

We then deduce the total potential energy:

$$I(U) = \frac{\mu}{2}\left\{\left(1 + \frac{U}{H}\right)^{-2} H + 2U - H\right\} + pU \tag{28}$$

By minimizing it, it is easy to find that U is the solution of the following equation:

$$K(U) = -p \tag{29}$$

where K is a non-linear function of U

$$K(U) = \mu\left[1 - \left(1 + \frac{U}{H}\right)^{-3}\right] \text{ if } U > -H \; ; \; K(U) = \mu\left[-1 - \left(1 + \frac{U}{H}\right)^{-3}\right] \text{ if } U < -H \tag{30}$$

These equations show that the equilibrium curve is made of two branches as shown in Fig. 3. On this figure, the solution of Eq. (29), with $-p$ equal to -1 MPa, is represented by a circle.

On the first branch, corresponding to U higher than $-H$, orientation is preserved. Indeed, it follows from Eqs. (24, 25) that the deformation gradient matrix is given by

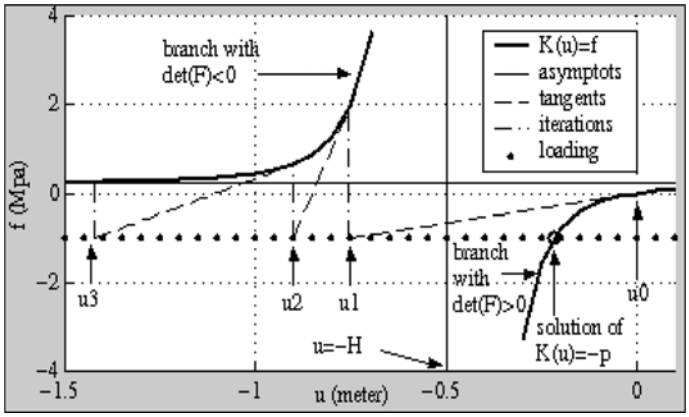

Fig. 3 Load-displacement curves

$$\mathbf{F} = \begin{pmatrix} 1 & 0 & 0 \\ 0 & 1 & 0 \\ 0 & 0 & 1+\dfrac{U}{H} \end{pmatrix} \tag{31}$$

The eigenvalues of **F** are thus

$$\lambda_1 = \lambda_2 = 0 \; ; \; \lambda_3 = 1 + \frac{U}{H} \tag{32}$$

We then deduce from Eq. (23) and Eq. (32) that

$$det(F) = 1 + \frac{U}{H} > 0 \tag{33}$$

On the other hand, the orientation preservation is lost on the second branch corresponding to U lower than $-H$. The vertical asymptote $u = -H$ thus constitutes the border separating the branch with a positive determinant, which corresponds to a physical solution, and the branch with a negative determinant. It is noted on Fig. 3 that incremental Newton-Raphson algorithm causes a discontinuous jump between these two branches if the loading increment is too large. Successive tangents allowing no return to the acceptable branch where the physical solution is located, the Newton-Raphson algorithm fails to converge (i.e., the iteration count is infinite or the iterative process stops with an error message).

Convergence is thus related to the position of intersection between tangent at the origin with the curve $K(U) = f$ and horizontal line of loading (Fig. 4). If this intersection is located at a first coordinate strictly higher than $-H$, the algorithm will converge. If the first coordinate of the intersection is lower or equal to $-H$, the algorithm will diverge.

The case corresponding to $-H$ thus separates convergence and divergence areas. It is shown in (Peyraut 2001) that the loading step number n associated with this specific case is given by

$$n = int\left[\frac{p}{3\mu}\right] + 1 \tag{34}$$

where *int* represents the integer part of a real number.

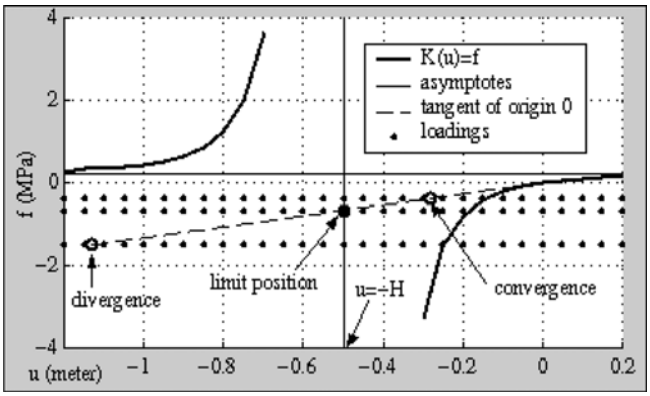

Fig. 4 Three possible cases for loading

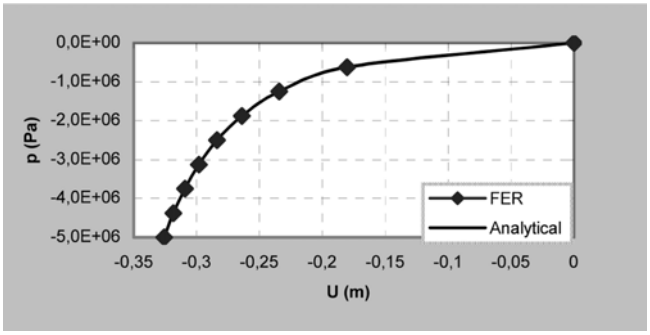

Fig. 5 Admissible load-displacement curve

It is also shown in the same reference that this loading step number is optimal because it gives the best compromise between two antagonistic objectives. The first objective is convergence of Newton-Raphson algorithm. To achieve this goal, the loading step number must be large. The second objective is minimization of time computation. For this purpose, the loading step number must be small since it represents the loading iteration count. Numerical simulation is performed with the data: μ = 220711.2 Pa; p = 5 MPa; H = 0.5 m. From Eq. (34), at least 8 load steps are necessary to obtain convergence of the solution. Fig. 5 shows the admissible branch of the load-displacement curve obtained analytically and numerically with n = 8.

Table 1 gives the eigenvalues of **F** calculated numerically when n = 7 and n = 8. One observes that with n = 7, there exists one negative eigenvalue. As mentioned in Section 4, the Newton-Raphson algorithm does not converge with n = 7.

Table 1 **F** eigenvalues

F eigenvalues	λ_1	λ_2	λ_3
numerical with n = 7 (FER)	1	1	–0.187159
numerical with n = 8 (FER)	1	1	0.0560817

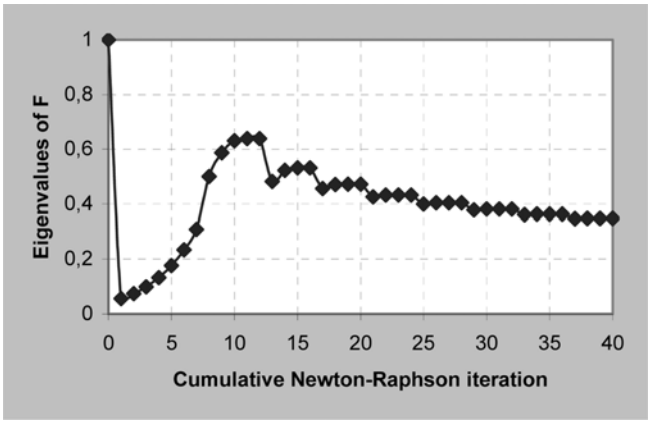

Fig. 6 Evolution of eigenvalues of **F**

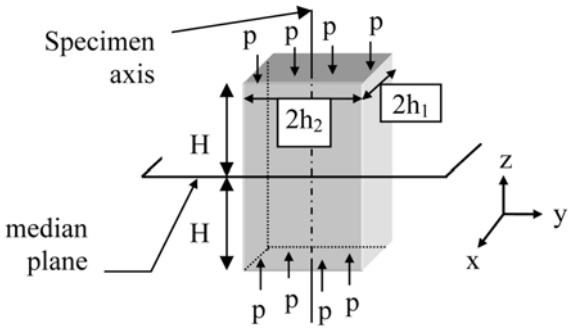

Fig. 7 Tensile ($p > 0$) or compressive ($p < 0$) loading

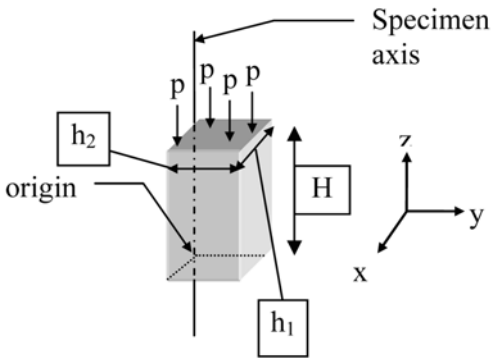

Fig. 8 1/8 of the structure

Fig. 6 shows the evolution of **F** eigenvalues with respect to the cumulative Newton-Raphson iteration in the case of $n = 8$. 40 iterations were performed to achieve the solution. It is worth noting that eigenvalue is reduced from 1 to 0.0560817 in the first iteration. As shown in Table 1, with $n = 7$, this value is reduced to −0.187159 and then the determinant of **F** becomes negative. The algorithm does not converge as predicted by the approach proposed in Section 4.

5.2 Three dimensional example

In this section, we study the three dimensional example of a rectangular specimen subjected to a uniform pressure p on the upper and lower sides (Fig. 7). A negative value of p is associated with a compressive loading and a positive value with a tensile loading. Dimensions of the rectangular specimen are $2h_1 \times 2h_2 \times 2H$.

Because of symmetry, only 1/8 of the structure (Fig. 8) is modeled. The origin is located at the intersection of the specimen axis and the median plane.

To take into account symmetry, we have selected the following boundary conditions:

$$u_x(0, y, z) = u_y(x, 0, z) = u_z(x, y, 0) = 0 \tag{35}$$

The displacements then depend on x, y and z in a linear form:

$$u_x(x) = \frac{U_x}{h_1}x \; ; \; u_y(y) = \frac{U_y}{h_2}y \; ; \; u_z(z) = \frac{U_z}{H}z \tag{36}$$

where U_x, U_y and U_z represent respectively the displacement on the lateral sides ($x = h_1$; $y = h_2$) and on the top side of the specimen ($z = H$).

As mentioned in section 5.1, the loss of orientation preservation can cause the incremental Newton-Raphson algorithm to diverge. In order to find the optimal incremental loading number n, which allows convergence without restarting, we proceed as in section 5.1. We first study the relation between displacements and loading. This relation can be obtained thanks to the minimization of the total potential energy:

$$U_x = \left\{ \pm \left(1 - \frac{p}{\mu} \right)^{\frac{1}{10}} - 1 \right\} h_1 \; ; \; U_y = \left\{ \pm \left(1 - \frac{p}{\mu} \right)^{\frac{1}{10}} - 1 \right\} h_2 \; ; \; U_z = \left\{ \pm \left(1 - \frac{p}{\mu} \right)^{-\frac{2}{5}} - 1 \right\} H \tag{37}$$

It can be easily deduced from Eq. (37) that

$$K_x(U_x) = p \; ; \; K_y(U_y) = p \; ; \; K_z(U_z) = p \tag{38}$$

where K_x, K_y and K_z are non-linear functions of U_x, U_y and U_z:

$$K_x(U_x) = \mu \left[1 - \left(1 + \frac{U_x}{h_1} \right)^{10} \right] \; ; \; K_y(U_y) = \mu \left[1 - \left(1 + \frac{U_y}{h_2} \right)^{10} \right] \tag{39}$$

$$K_z(U_z) = \mu \left[1 - \left(1 + \frac{U_z}{H} \right)^{-\frac{5}{2}} \right] \text{ if } U_z > -H \; ; \; K_z(U_z) = \mu \left[1 - \left(-1 - \frac{U_z}{H} \right)^{-\frac{5}{2}} \right] \text{ if } U_z < -H \tag{40}$$

The curves of Eqs. (39,40) are represented on Figs. 9 and 10 with the following numerical data: H = 25 cm ; h_1 = 2.5 cm ; h_2 = 1.25 cm ; μ = 220711.2 Pa. We notice that these curves are perfectly correlated with numerical results performed with the finite elements software FER. The curve of U_y vs. p is not represented because it has exactly the same form as U_x.

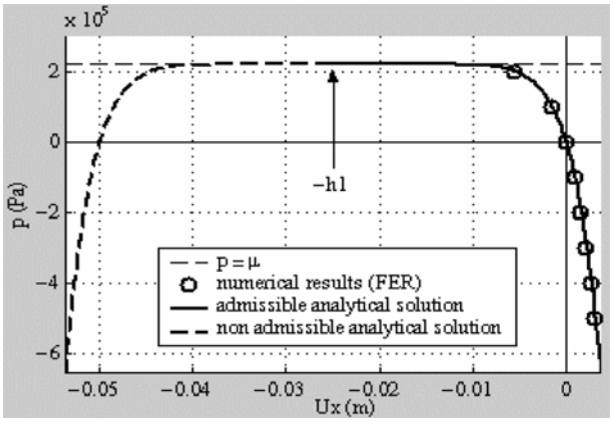

Fig. 9 Horizontal displacement $U_x = u_x(h_1)$ vs loading p

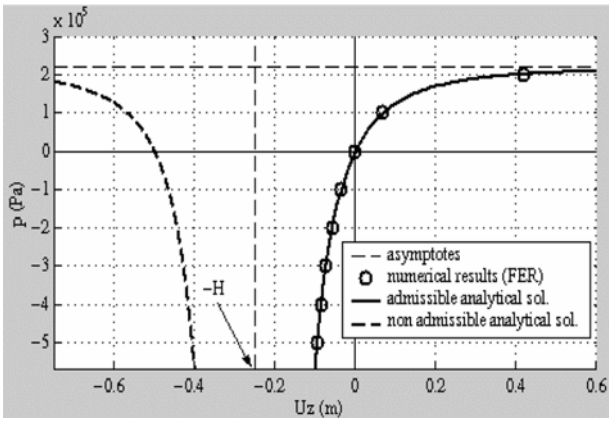

Fig. 10 Vertical displacement $U_z = u_z(H)$ vs loading p

Fig. 10 shows that the equilibrium curve related to the vertical displacement is made of two branches. The admissible branch is represented by the solid line and the non-admissible branch by the curve in dotted lines. On the non-admissible branch, corresponding to U_z lower than $-H$, the orientation preservation is lost. Indeed, it follows from Eq. (36) that the deformation gradient matrix is

$$\mathbf{F} = \begin{pmatrix} 1 + \dfrac{U_x}{h_1} & 0 & 0 \\ 0 & 1 + \dfrac{U_y}{h_2} & 0 \\ 0 & 0 & 1 + \dfrac{U_z}{H} \end{pmatrix} \tag{41}$$

We deduce from Eq. (41) the eigenvalues of **F**:

$$\lambda_1 = 1 + \frac{U_x}{h_1} \; ; \; \lambda_2 = 1 + \frac{U_y}{h_2} \; ; \; \lambda_3 = 1 + \frac{U_z}{H} \tag{42}$$

If U_z is lower than $-H$, the third eigenvalue of **F** is negative. According to the conclusion of Section 4, the orientation is not preserved. As in section 5.1, the vertical asymptote $U_z = -H$ constitutes a border between an admissible branch and a branch which is not. It is shown in (Peyraut 2003b) that the optimal loading step number, which allows convergence with a minimal computation cost, can be chosen by using the border between these two branches

$$n = int\left[-\frac{p}{E}\right] + 1 \tag{43}$$

where *int* represents the integer part of a real number.

In order to correlate Eq. (43), numerical simulations have been performed with the data: E = 551778 Pa; p = −6014380.2 Pa; H = 0.25 m, h_1 = 0.025 m, h_2 = 0.0125 m. The pressure p has been chosen such as the ratio $-p/E$ is equal to 10.9. From Eq. (43), at least 11 load steps are necessary to

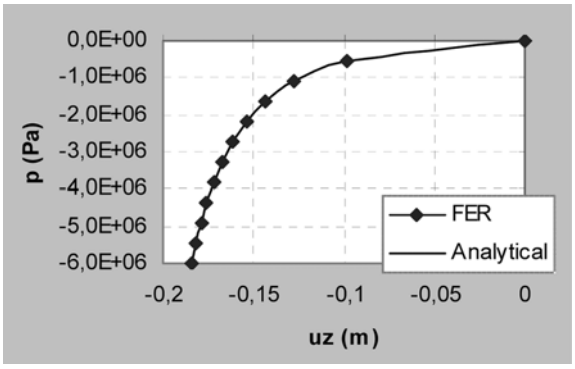

Fig. 11 Admissible load-displacement curve

Table 2 **F** eigenvalues

F eigenvalues	λ_1	λ_2	λ_3
numerical with n = 10 (FER)	1.44574	1.44574	–0.214827
numerical with n = 11 (FER)	1.24773	1.24773	0.00909091

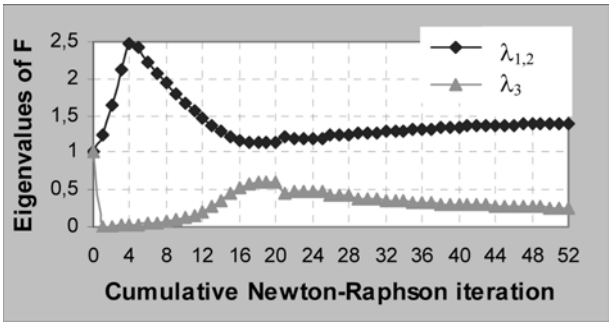

Fig. 12 Evolution of **F** eigenvalues

obtain the convergence of the solution. Fig. 11 shows the admissible branch of load-displacement curves obtained analytically and numerically with n = 11.

Table 2 gives the eigenvalues of **F** calculated numerically when n = 10 and n = 11. One observes that with n = 10, there exists at least one negative eigenvalue. As mentioned in Section 4, the Newton-Raphson algorithm does not converge with n = 10.

Fig. 12 shows the evolution of eigenvalues of **F** with respect to the cumulative Newton-Raphson iteration in the case of n = 11. 52 iterations were performed to achieve the solution. It is worth noting that the eigenvalue is reduced from 1 to 0.0090909 in the first iteration. As shown in Table 2, with n = 10, this value is reduced to –0.214827 and then the determinant of **F** becomes negative. The algorithm does not converge as predicted by the approach proposed in Section 4. It is also noticed that the first and second eigenvalues are identical because of the symmetry of the problem.

6. Conclusions

In this paper, we have shown that the orientation preservation violation constitutes a potential cause of divergence for the Newton-Raphson algorithm. We also show that a control by eigenvalues of the deformation gradient matrix F is efficient to detect a loss of orientation preservation.

These points are successfully shown in two cases. Convergence can be obtained by choosing a sufficiently small the initial load step number. For the chosen examples, this number is analytically determined and validated by numerical results.

For a more general case, there does not exist, a priori, analytical formulas allowing the choice of the initial load step. In this case, a new approach is proposed which consists of integrating numerically the risks of divergence related to the orientation preservation violation in a traditional Newton-Raphson algorithm. This integration is achieved by controlling the eigenvalues of the deformation gradient matrix and by restarting the Newton-Raphson procedure. Further studies and software development are being undertaken for implementing an automatic process to determine the optimum load step number without restart.

References

Bathe, K.J. and Bolourchi, S. (1979), "Large displacement analysis of three-dimensional beam structures", *Int. J. Num. Meth. Engng.*, **14**, 961-986.

Belytschko, T., Liu, W.K. and Moran, B. (2000), *Nonlinear Finite Elements for Continua and Structures*, Chichester (UK), Wiley.

Blatz, P.J. and Ko, W.L. (1962), "Application of finite elastic theory to the deformation of rubbery materials", *Transactions of the Society of Rheology*, **6**, 223-251.

Ciarlet, P.G. (1988), *Mathematical Elasticity*, Vol. 1 : *Three-dimensional Elasticity*, North-Holland.

Horgan, C.O. (1996), "Remarks on ellipticity for the generalized Blatz-Ko constitutive model for a compressible nonlinearly elastic solid", *Journal of Elasticity*, **42**, 165-176.

Peyraut, F. (2003), "Orientation preservation and Newton-Raphson convergence in the case of an hyperelastic sphere subjected to an hydrostatic pressure", *Comput. Methods Appl. Mech. Engrg.*, **192**, 1107-1117.

Peyraut, F. and Labed, N. (2001), "Préservation de l'orientation et convergence de Newton-Raphson avec le modèle hyperélastique compressible de Blatz-Ko", *Revue Européenne des Eléments Finis*, **10**, 595-605.

Peyraut, F. and Labed, N. (2003), "Condition de préservation de l'orientation – Application en hyperélasticité compressible", *Revue Européenne des Eléments Finis*, **12**, 99-116.

Wineman, A.S. and Waldron, W.K. (1995), "Normal stress effects induced during circular shear of a compressible non-linear elastic cylinder", *Int. J. Non-Linear Mechanics*, **30**, 323-339.

Wood, R.D. and Zienkiewicz, O.C. (1977), "Geometrically nonlinear finite element analysis of beams, frames, arches and axisymmetric shells", *Comput. Struct.*, **7**, 725-735.

Appendix: Reversal problem

Usually, the orientation preserving problem occurs with a negative volume. But it can also occur in the case of a positive volume but a negative area. This leads to the reversal problem which is not physically meaningful. To explain this problem let us consider three infinitesimal and orthogonal vectors $\partial\mathbf{a}$, $\partial\mathbf{b}$ and $\partial\mathbf{c}$ (Fig. A1). In order to simplify the presentation, assume that these three vectors, whose lengths $\|\partial\mathbf{a}\|$, $\|\partial\mathbf{b}\|$ and $\|\partial\mathbf{c}\|$ are strictly positive, are parallel to the axes

$$\partial\mathbf{a} = \|\partial\mathbf{a}\|\mathbf{e}_1 \ ; \ \partial\mathbf{b} = \|\partial\mathbf{b}\|\mathbf{e}_2 \ ; \ \partial\mathbf{c} = \|\partial\mathbf{c}\|\mathbf{e}_3 \tag{A.1}$$

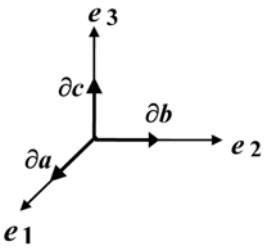

Fig. A1 Three infinitesimal and orthogonal vectors parallel to the axes

Let us consider the undeformed surface S_0 supported by $\partial\mathbf{a}$ and $\partial\mathbf{b}$ and oriented by the normal

$$\mathbf{n}_0 = \frac{\partial\mathbf{a} \wedge \partial\mathbf{b}}{\|\partial\mathbf{a} \wedge \partial\mathbf{b}\|} = \mathbf{e}_3 \tag{A.2}$$

The deformed surface S is then supported by the vectors $\mathbf{da}$ and $\mathbf{db}$

$$\mathbf{da} = \mathbf{F}\partial\mathbf{a} = \lambda_1\|\partial\mathbf{a}\|\mathbf{e}_1 \; ; \; \mathbf{db} = \mathbf{F}\partial\mathbf{b} = \lambda_2\|\partial\mathbf{b}\|\mathbf{e}_2 \tag{A.3}$$

Moreover, this surface is directed by the deformed normal defined by

$$\mathbf{n} = \frac{\mathbf{da} \wedge \mathbf{db}}{\|\mathbf{da} \wedge \mathbf{db}\|} = \text{sign}(\lambda_1\lambda_2)\mathbf{n}_0 \tag{A.4}$$

Lastly, as λ_1 and λ_2 are negative, the product of λ_1 by λ_2 is positive. The deformed and undeformed normals are then identical:

$$\mathbf{n} = \mathbf{n}_0 \tag{A.5}$$

Surfaces S and S_0 have thus the same normal. In addition, according to (A.1) and (A.3), directions of $\partial\mathbf{a}$ and $\mathbf{da}$ are opposite. We have the same conclusion concerning $\partial\mathbf{b}$ and $\mathbf{db}$. It means that surface S results from S_0 by a reversal procedure (Fig. A2). This reversal procedure has no physical meaning. It then should be proscribed.

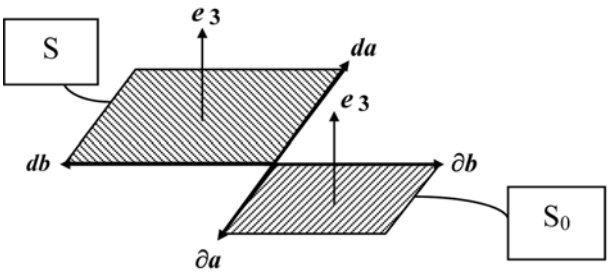

Fig. A2 Surface reversal